PHYSICAL REVIEW D

PARTICLES AND FIELDS

THIRD SERIES, VOLUME 31, NUMBER 1 1 JANUARY 1985

Study of quark fragmentation in e^+e^- annihilation at 29 GeV: Global jet parameters and single-particle distributions

D. Bender,[a] M. Derrick, E. Fernandez,[b] R. Fries,[c] G. Gieraltowski,[d] L. Hyman,[d] K. Jaeger,[a] R. Klem,[d] P. Kooijman, J. S. Loos, F. LoPinto,[e] B. Musgrave, L. E. Price, J. Schlereth, P. Schreiner,[d] R. Singer,[d] K. Sugano, T. Trinko,[f] M. Valdata-Nappi,[g] C. Ward,[d] and J. M. Weiss
Argonne National Laboratory, Argonne, Illinois 60439

S. Ahlen, G. Baranko,[h] P. Baringer, D. Blockus, B. Brabson, M. Daigo,[i] S. Ems,[j] G. E. Forden,[k] S. W. Gray, J.-P. Guillaud,[l] C. Jung, H. Neal,[m] H. Ogren, D. Rust, and P. Smith
Indiana University, Bloomington, Indiana 47401

C. Akerlof, J. Chapman, D. Errede, N. Harnew,[n] P. Kesten, S. Kooijman, D. I. Meyer, D. Nitz, D. Rubin,[o] A. A. Seidl, R. Thun, and M. Willutzky
University of Michigan, Ann Arbor, Michigan 48109

I. Beltrami, R. DeBonte, K. K. Gan, D. Koltick, F. Loeffler, U. Mallik, R. McIlwain, D. H. Miller, C. R. Ng, P. P. Ong,[p] L. K. Rangan, E. I. Shibata, R. Stevens,[q] R. J. Wilson,[r] and D. E. Wood[s]
Purdue University, West Lafayette, Indiana 47907

B. Cork
Lawrence Berkeley Laboratory, Berkeley, California 94720

L. Keller and J. Va'vra
Stanford Linear Accelerator Center, Stanford, California 94305

(Received 21 May 1984)

In this paper, results are presented from a study of the hadronic final states in e^+e^- annihilation at 29 GeV. The data were obtained with the High Resolution Spectrometer (HRS) at the SLAC PEP e^+e^- colliding-beam facility. The results are based on 6342 selected events corresponding to an integrated luminosity of 19.6 pb^{-1}. The distributions of the events in sphericity (S), thrust (T), and aplanarity (A) are given and compared to other e^+e^- data in the same energy range. We measure $\langle S\rangle = 0.130 \pm 0.003 \pm 0.010$ and $\langle 1-T\rangle = 0.100 \pm 0.002$. The sphericity distribution is compared to sphericity measurements made for beam jets in hadronic collisions as well as jets studied in neutrino scattering. The data sample is further reduced to 4371 events with the two-jet selections, $S \leq 0.25$ and $A \leq 0.1$. The single-particle distributions in the longitudinal and transverse directions are given. For low values of the momentum fraction ($z = 2p/W$), the invariant distribution shows a maximum at $z \sim 0.06$, consistent with a QCD expectation. The data at high Feynman x (x_F) show a distribution consistent with being dominated by a $(1-x_f)^2$ variation for the leading quark-meson transition. The rapidity distribution shows a shallow central minimum with a height $(1/N_{ev}dN^h/dY \mid_{Y=0} = 2.3 \pm 0.02 \pm 0.07$. The mean charged multiplicity is measured to be $\langle n_{\rm ch}\rangle = 13.1 \pm 0.05 \pm 0.6$. The mean transverse momentum relative to the thrust axis $\langle p_T\rangle$ rises as a function of z to a value of 0.70 ± 0.02 GeV/c for $z > 0.3$. The distributions are compared to those measured in other reactions.

INTRODUCTION

The study of multiparticle final states in high-energy reactions has a long history. In hadronic interactions the limited transverse momentum characteristic of the soft collisions that make up most of the cross section means that the particles are emitted in jets along the beam directions. Although there is no quantitative theory of the processes responsible, detailed phenomenological studies have been made with data from Fermilab[1] and CERN.[2]

Hadronic jets have also been found to dominate all short-distance interactions,[3] such as e^+e^- annihilation, deep-inelastic lepton-nucleon scattering, and high-transverse-energy hadron collisions both at the highest CERN ISR energy and at the CERN SPS collider energy. In these hard processes, jet production is generally regarded as a manifestation of pointlike constituents or partons, and the dynamics of the fundamental processes can be described by quantum chromodynamics (QCD). In terms of partons the jets observed in e^+e^- annihilation, in deep-inelastic scattering, and in pp collisions at the ISR are expected to result from quark fragmentation,[4] whereas the jets[5] seen at the CERN $\bar{p}p$ collider at high transverse energy are expected to be mostly from gluon fragmentation.[6]

The observation of three-jet events in high-energy

e^+e^- annihilations is clear qualitative evidence for the correctness of the QCD framework.[3] The dominant processes leading to the hadronic final states are

$$e^+e^- \rightarrow q\bar{q} \rightarrow \text{hadrons}\ , \quad (1)$$

$$e^+e^- \rightarrow q\bar{q}g \rightarrow \text{hadrons}\ . \quad (2)$$

At low center-of-mass energy ($W \leq 10$ GeV), the contribution of gluon bremsstrahlung is expected to be negligible. With increasing energy, however, reaction (2) becomes more and more important, leading to an increase in the transverse momentum and finally to an explicit three-jet structure. Although detailed analyses of such reactions have provided much supporting evidence for QCD, the dominance of nonperturbative effects has not yet allowed an unambiguous, single, quantitative test of the theory.

The theoretical situation in low-p_T hadron physics is much less clear. There have been some attempts to extend the QCD ideas into this kinematic regime,[7] in which the final states are thought to result from a superposition of several contributions arising from the multiquark nature of the interaction. Nevertheless, there are some experimental similarities between the properties of low-p_T hadron jets and those seen in hard processes.[8–12]

One essential difficulty of such comparisons is the presence in hadronic reactions of sizable elastic and diffractive components and so-called leading-particle effects, absent in e^+e^- annihilation into hadrons. The separation of diffractive and nondiffractive components cannot be done uniquely and, in addition, even the appropriate comparison energy scale is not unambiguously defined. Since the available center-of-momentum (c.m.) energy (W) is dominant in determining the overall character of the events,[13] an appropriate energy definition is essential if quantitative comparisons are to be made between data sets from different reactions. A second difference is that in e^+e^- data, almost half of the cross section leads to final states resulting from the fragmentation of the heavy quarks (c,b), in contrast to hadronic interactions, where such production is at the fraction of a percent level.

In this paper we present our results on the global jet measures and the single-particle distributions in e^+e^- annihilation into hadrons at $W=29$ GeV.[14] Although three-jet events are important[15] in the PEP energy range, in this initial report we confine our attention to an enriched two-jet sample, which we use to measure properties of quark fragmentation. We make a number of empirical comparisons with data from other reactions in order to show which features are universal and which are intrinsic to simple quark fragmentation. It is necessary to understand the fragmentation process before definitive conclusions can be made about the parton-level processes, and so we consider studies such as are reported in this paper to be an essential preliminary to the next stage of comparisons with QCD.

APPARATUS

The results are based on the hadronic annihilation events collected by the High Resolution Spectrometer (HRS) at the SLAC e^+e^- storage ring PEP. The events were collected at c.m. energy $W=29$ GeV, and the data sample corresponds to an integrated luminosity of 19.6 pb^{-1}.

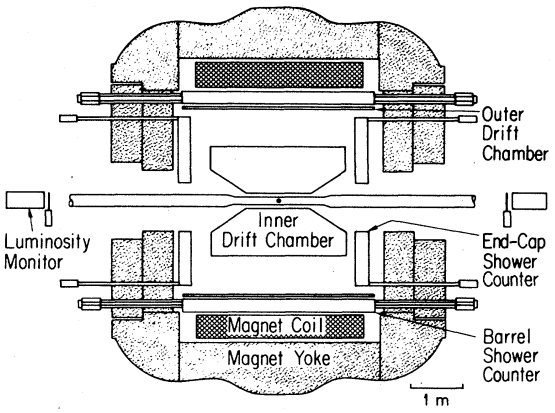

FIG. 1. Cross-section view of the HRS as used in the present experiment.

The HRS, shown in Fig. 1, has been described in detail elsewhere.[16] We list here only the points relevant to this analysis. The detector measures charged secondaries over a solid angle of approximately 90% of 4π. The momentum resolution of high-momentum tracks is $\sigma_p = 1\times10^{-3}p^2$ (p and σ_p in GeV/c) for $\sim$60% of 4π and $\sigma_p < 5\times10^{-3}p^2$ for the remaining 30% of the tracking solid angle. The tracking system is surrounded by calorimetric shower counters consisting of lead/scintillator sandwiches, which also give time-of-flight information. The positions of showers are measured by a set of proportional tubes. The detector was triggered by requiring at least one of the following conditions to be satisfied: (a) three or more charged tracks, (b) two charged tracks plus an in-time requirement with the beam crossing, (c) one charged track plus ≥ 2.4 GeV of neutral energy deposited in the calorimeters, or (d) more than 4.8 GeV of neutral energy deposited in the calorimeters.

Both the vacuum pipe of PEP and the inner cylinder of the drift chamber are made of beryllium in order to minimize photon conversions and reduce the multiple scattering of the charged tracks. The total detector thickness from the annihilation point to the outer tracking layer was $0.02X_0$.

DEFINITION OF VARIABLES

The global properties of the events were studied in terms of the jet variables sphericity (S), aplanarity (A),

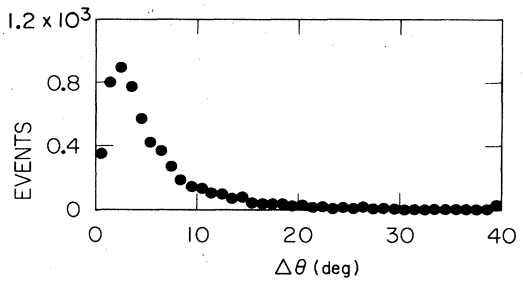

FIG. 2. Angle between the calculated thrust and sphericity axes for the selected events.

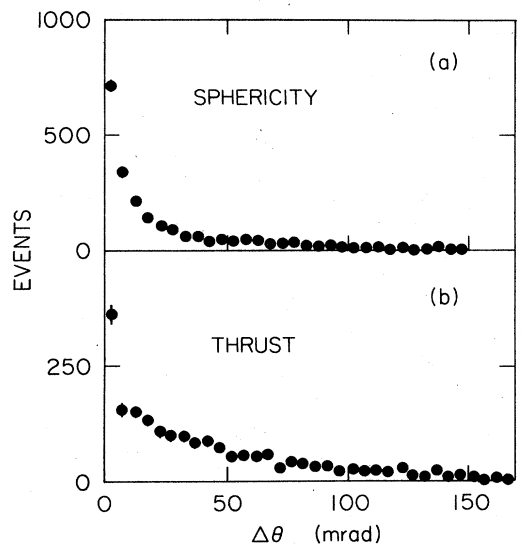

FIG. 3. Net change ($\Delta\theta$) in (a) the S axis, and (b) the T axis after passing MC-generated events through the detector simulation.

and thrust (T).[17] The quantities $(p_{T_{\text{out}}})^2$ and $(p_{T_{\text{in}}})^2$, are, respectively, the square of the momentum normal to and in the event plane, but normal to the S axis.

The jet axes, as measured by sphericity and thrust, do not correlate exactly with the parton direction. As a measure of this uncertainty, we show in Fig. 2 the experimental distribution in the angle between the T and S axes. The distribution is centered at 3° with a width of 2°, although there are some events in a long tail extending as far as 20°. This difference does not result from the reconstruction errors on the tracks. The axis uncertainty coming from track errors has been estimated by using the Monte Carlo (MC) simulation of the experiment discussed in the next section. The results are shown in Figs. 3(a) and 3(b) for sphericity and thrust, respectively. The change of the axes coming from the track errors is typically less than 10 mr although with some events at much higher values.

Since the sphericity is more sensitive to background, the thrust axis is used to define the jet axis: positive thrust is chosen along the positive Z direction which is the direction of the incident positron beam. The quarks produced in the primary reaction $e^+e^-\rightarrow q\bar{q}$ fragment into hadrons, each of which takes a fraction of the quark energy. As a measure of this fraction, we use the variable $z=2p/W$, where p is the particle momentum, since it can be measured without knowing the particle species. Other measures of the longitudinal distribution of the hadrons are Feynman x (x_F), where $x_F=2p_L/W$ and rapidity (Y),

$$Y=\tfrac{1}{2}\ln(E-p_L)/(E+p_L)\ ,$$

where p_L is the component of momentum parallel to the thrust axis. In measuring these variables, we use a c.m.-energy value of 29 GeV.

The fragmentation function for a quark of type q to produce a hadron of type h is defined as the hadron density per unit of z:

$$D^h(z)=\frac{1}{N_{\text{ev}}}\frac{dN^h}{dz}\ .$$

The invariant x_F distribution $F(x_F)$ is given by

$$F(x_F)=\frac{1}{\pi}\frac{1}{N_{\text{ev}}}\frac{2E}{W}\frac{dN^h}{dx_F}$$

$$\simeq\frac{x_F}{\pi}D^h(x_F)\ .$$

for large x_F.

In e^+e^- experiments, the different quark species are produced with relative weights given simply by the square of their charges. The fragmentation function we report is therefore such an average over the u, d, c, s, and b quarks.

DATA SELECTION

One-photon-annihilation sample

To select the hadronic data sample and to discriminate against backgrounds, several cuts were applied.

To remove $\tau^+\tau^-$ pair events and to minimize beam-gas interactions as well as backgrounds from two-photon scattering, we required the events to have (a) five or more charged tracks, (b) a vertex constrained to the interaction point to within 2 cm in X,Y radius and 8 cm in Z along the beam direction, (c) a visible charged momentum of $\sum|\vec{p}|\geq 5.8$ GeV/c, and (d) more than 1.5 GeV of energy deposited in the central electromagnetic calorimeter. Minimum and maximum momentum values for any accepted track were 0.1 and 15 GeV/c, respectively.

Although some particle identification was available from time of flight, we assigned all particles the pion mass for this study.

To minimize geometrical losses of tracks at small angles to the beam, a fiducial cut was applied requiring that the thrust axis of the event have an angle greater than 45° with respect to the beam axis. These cuts yield a sample of 6342 events that we consider to be due to one-photon annihilation.

Two-jet events

In order to choose an enriched sample of $q\bar{q}$ fragmentation events, we selected events in a specified region of the sphericity-aplanarity space. The distribution of hadronic events in these variables is shown in Fig. 4. The defini-

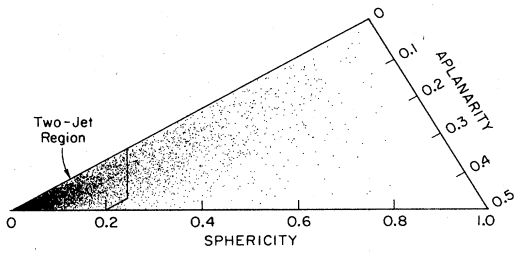

FIG. 4. Event distribution in the sphericity: aplanarity space. The region used to select a two-jet sample is indicated.

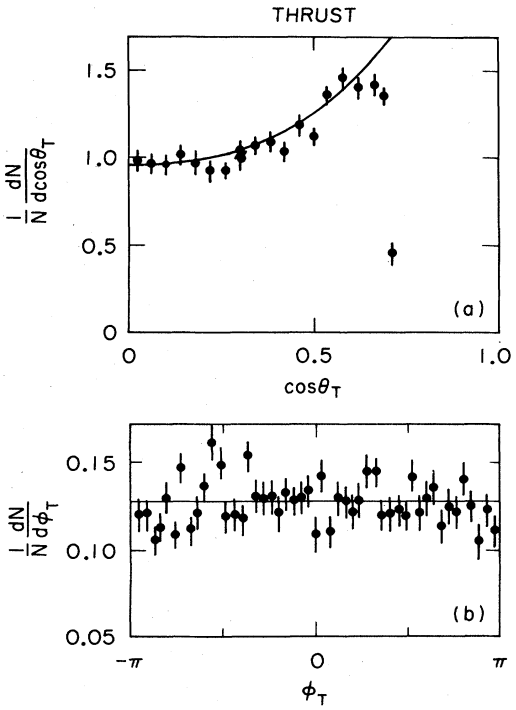

FIG. 5. Distribution in polar angle (θ_T) and azimuthal angle (ϕ_T) of the thrust axis for the two-jet events. The line shows the expected shapes as predicted by the MC simulation.

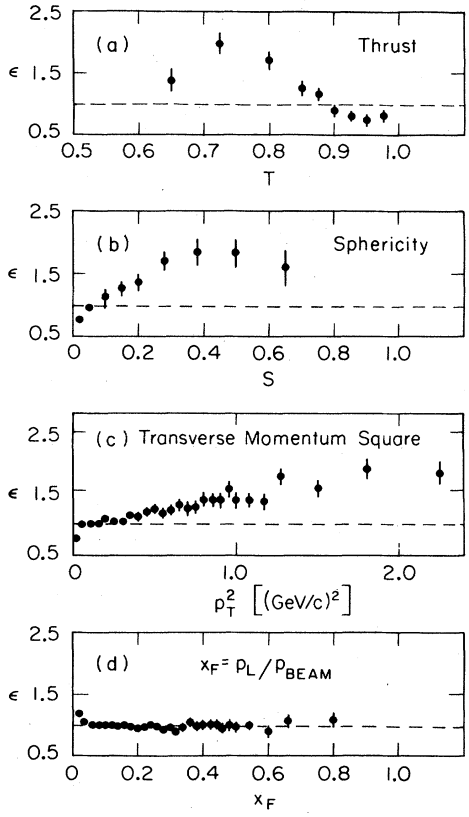

FIG. 6. Correction factors to the different variables as estimated using the MC simulation. (a) Thrust, (b) sphericity, (c) p_T^2, and (d) x_F.

tion of a two-jet event is arbitrary because gluon emission is a radiative process, but we define a collimated ($S \leq 0.25$) and planar ($A \leq 0.10$) sample as two-jet events. The distributions in azimuthal ϕ_T and polar angle θ_T of the T axis for the two-jet events shown in Fig. 5 are in good agreement with the expected underlying $q\bar{q}$ behavior; isotropic and $(1+\cos^2\theta)$, respectively. The lines on Fig. 5 show the predicted T-axis distribution from the MC simulation.

Since only the charged particles are used for the present study, we further require that both jets have more than 2 GeV/c of momentum in charged particles. With these selections, the data set consists of 4371 events.

If we further define the "three-jet" events as those with $S > 0.25$ and $A \leq 0.1$, our data, corrected for efficiencies, measure a ratio for the three-jet events to the total one-photon-annihilation events of about 0.13.

CORRECTION FACTORS

In order to measure the effects on the data of the selection criteria, quantify the smearing introduced by measuring errors, and determine the efficiency of the track recognition and reconstruction, the experiment has been simulated in a Monte Carlo program.[18] The results of this simulation give a good representation of the data and so the correction factors are based on a realistic model. We do not, in this paper, use our data to discriminate amongst the several MC simulations of the e^+e^- annihilation process that have been discussed in the literature.[19]

From our MC study we found that the overall single track-finding efficiency was 90% and the fraction of one-photon-annihilation events in the fiducial volume that satisfied the selection criteria was 94%. The more stringent criteria applied to select the two-jet events reduced the detection efficiency for that sample to 82%. The track definitions applied accepted most of the charged hadrons from K_S^0 and Λ decay, as well as a small contamination from γ conversion and Dalitz-pair production. Appropriate corrections are made for the additional tracks that come from these sources.

All of the measurements presented are corrected for efficiencies and resolution effects. The correction factors in the different kinematic variables are measured by the ratio of the MC-generated distribution to the same distribution after the MC data have passed through the detector simulation and event reconstruction programs. The correction includes the effects of initial-state electromagnetic radiation. The principal effect of this radiation is a small reduction in W to ~ 27.3 GeV.

The correction factors depend strongly on the kinematic variable. As shown in Fig. 6, the corrections to the thrust and sphericity variables, for example, can be as high as 1.5—2 in some regions, since the correction depends on the combined effect of the smearing of the axes as well as on the particular values of the variable. A similar effect is present in the p_T^2 variable. The longitudinal

variables, one the other hand, are quite insensitive except for the lowest and highest values.

The systematic error on the correction factors and thus on our measurements is dependent on how well the data are represented by the MC-generated events. The magnitude of the systematic error is estimated using an iterative procedure, assuming that each variable factorizes. The systematic error is quoted whenever it is significant with respect to the statistical error, but is not shown in the figures.

RESULTS

General properties of the events

Using the MC simulation, including initial-state radiation, we have estimated the correction factors coming from the above-mentioned cuts on our sample of hadronic events. Detailed comparisons have been made between the MC simulation and many aspects of the data.

The two-dimensional distribution in total charged momentum $\sum |p|$ and the total z component $\sum p_z$ for the 6342 events in the one-photon-annihilation sample is shown in Fig. 7. Two photon interactions populate the region at low $\sum |p|$ and high $\sum p_z$; our cuts, especially the T-axis selection, are effective in reducing this background. The vertex cut reduces the beam-gas background. We expect the remaining background to be flat in $\sum p_z$, consistent with the agreement between the MC simulation and the data in this variable. By restricting the data sample to very high quality tracks and correcting the distribution in $\sum |p|$ using the MC simulation, we conclude that some background exists for low values of this variable. The shape of this background, which is shown by the dotted line in the $\sum p$ projection on Fig. 7, is obtained from this study. The full line on the $\sum p$ projection shows our best estimate of the true shape of this distribution. From these studies, we measure a residual contamination in the data sample of $(12\pm4)\%$.

We have studied the effect of this background on the kinematic variables presented in this paper by selecting a subsample of events with thrust axis $>70°$ with respect to the e^+e^- beam directions. These events, which have lower background, give the same results within errors. A data sample selected with $\sum |p| \gtrsim 15$ GeV is free of background, but the MC corrections are large. The errors

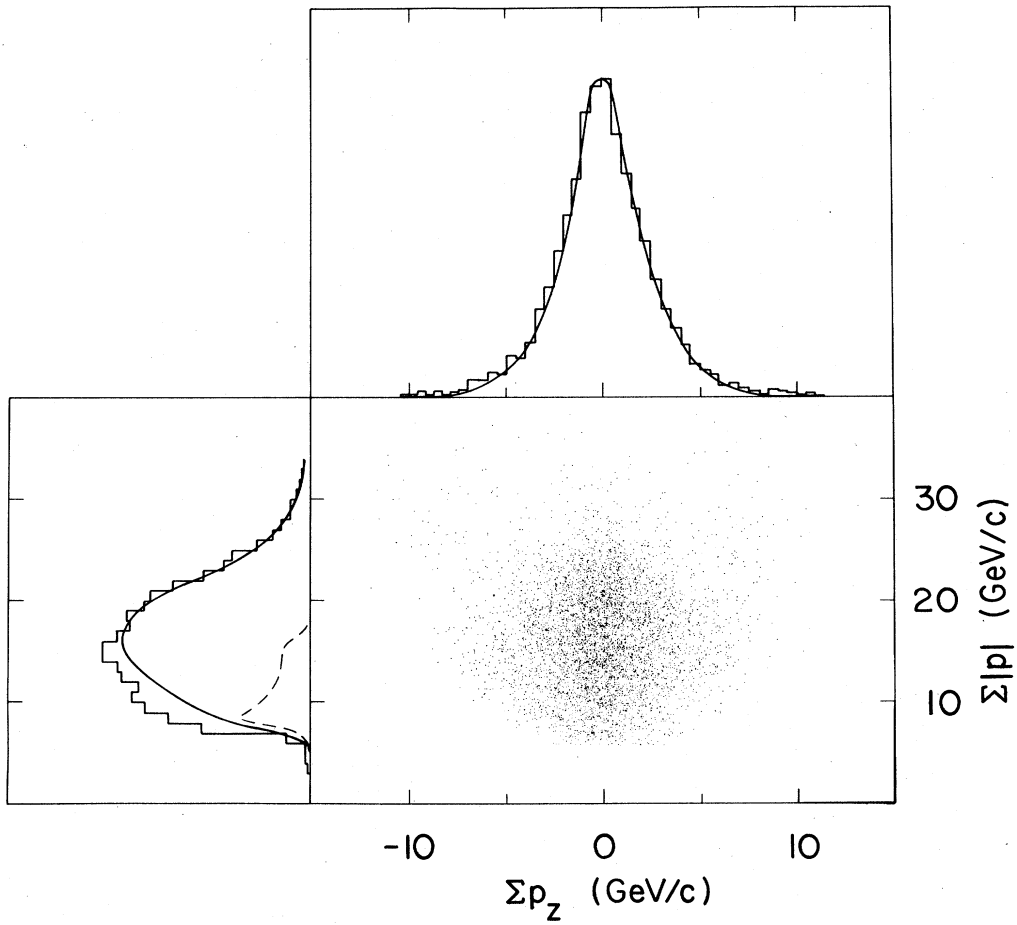

FIG. 7. Distribution in total charged momentum $\sum |p|$ and z component $\sum p_z$ for the one-photon-annihilation events. The full curves on the projections show the MC predictions. The dashed curve shows our estimate of the background as reflected in the $\sum |p|$ projection.

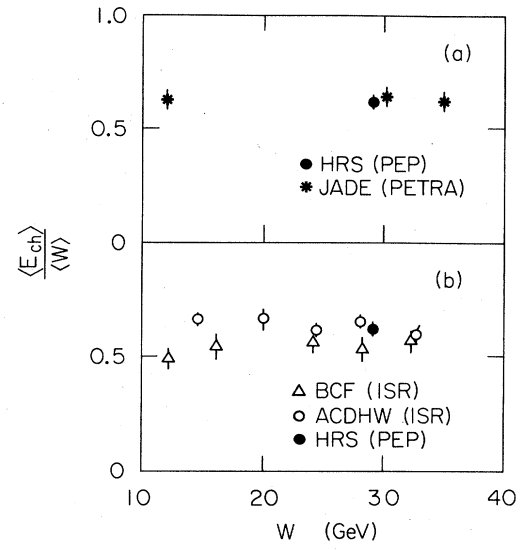

FIG. 8. Fractional charged energy as a function of c.m. energy W, compared to (a) the JADE e^+e^- measurements and (b) two experiments measuring pp beam jets at the ISR.

quoted on the different variables include the uncertainties coming from the background.

The MC simulation measures the overall acceptance for the one-photon-annihilation sample within our cuts to be 55%. Using this acceptance, the integrated luminosity of 19.6 pb^{-1} measured from the large-angle Bhabha scattering,[16] and the radiatively corrected point cross section of $\sigma_{\mu\mu}=0.122$ nb, we can measure the ratio R of the hadronic annihilation cross section to the point cross section. We find an hadronic cross section of 0.518 nb and so an R value of 4.2. Although the statistical error is small, a systematic error of 7% is estimated from uncertainties in the acceptance calculation and in the background evaluation. This value is in agreement with QCD expectation and with the precise measurement of $3.89\pm0.04\pm0.1$ made by the MAC collaboration[20] at the same 29-GeV c.m. energy.

The mean visible energy defined assuming all of the charged particles are pions is $\langle E_{\rm ch}\rangle=16.5\pm0.07$ GeV, giving a ratio $\langle E_{\rm ch}\rangle/W=0.570\pm0.003$. This value becomes $0.620\pm0.004\pm0.020$ after corrections are made for initial-state radiation, for photon conversions, for geometrical losses, and for the masses of the heavier particles that are produced in the annihilation process.

The value for the fractional charged momentum is in agreement with the measurements of the JADE group[21] who measured both the charged particles and the photon energies as seen in Fig. 8(a).

In Fig. 8(b) we show the results of two groups that have reported low-p_T proton-proton scattering data at $W=63$ GeV.[8,12] Different techniques were used to remove the leading-particle effects. The Bologna-CERN-Frascati (BCF) collaboration removes one leading prong, retaining $\sim10\%$ of the unbiased inelastic triggers, and they then analyze the remaining hadrons which are in the same hemisphere as the leading proton. The Ames-CERN-Dortmund-Heidelberg-Warsaw (ACDHW) collaboration[12] selects only those events with two leading protons and then analyze the hadrons remaining after removing the leading protons. Both groups adjusted the hadronic-energy values to compensate for these selections.

The BCF data (open triangles) lie systematically below those of the ACDHW group (open circles). This variation among data taken at the same energy, at the same accelerator, with almost the same apparatus and analyzed in similar ways, points up the experimental difficulties in establishing an hadronic-data sample and provides a measure of the precision with which we can expect to compare hadronic results from colliding-beam machines with e^+e^- data.

Global jet measures

In Fig. 9(a), we show the sphericity distribution of the one-photon-annihilation sample compared with data taken at DESY PETRA at $W\simeq30$ GeV.[22] The agreement between our data and that of the TASSO collaboration is good.

Our results are also compared with the pp data of the ACDHW collaboration[12] in a similar interval of hadronic

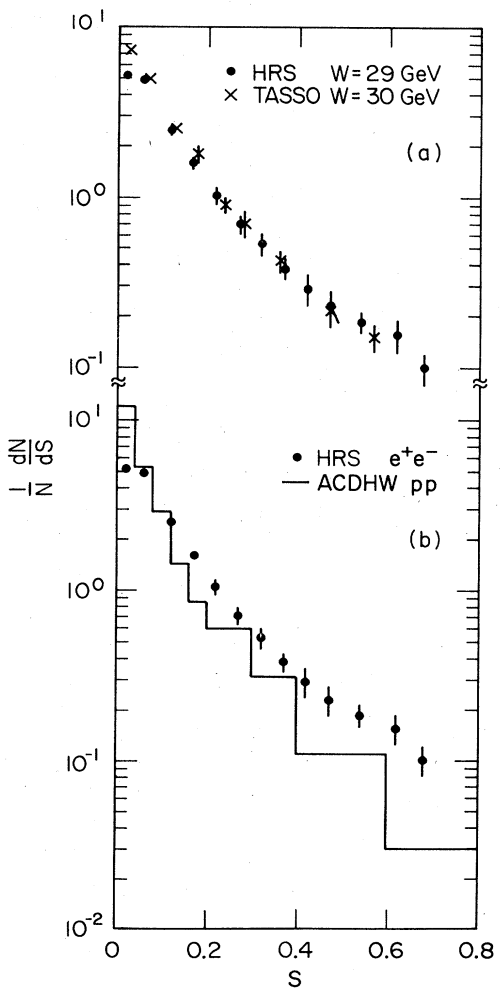

FIG. 9. (a) Sphericity distribution compared to the TASSO measurements. (b) Comparison of our sphericity distribution with that of the ACDHW collaboration.

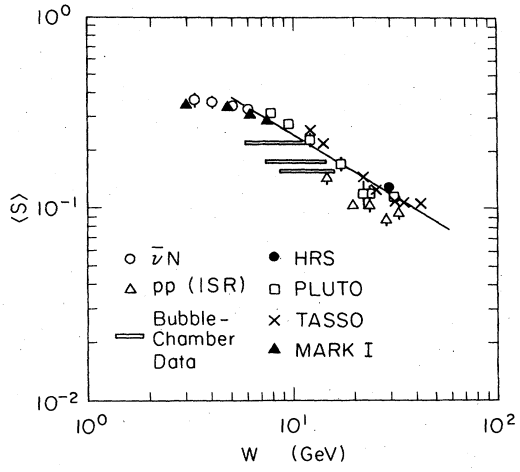

FIG. 10. Mean sphericity $\langle S \rangle$ as a function of c.m. energy W for various reactions. The line shows the function $\langle S \rangle = 1.07 W^{-0.645}$ which fits the e^+e^- data from the Mark I, PLUTO, TASSO, and HRS detectors for $W > 5$ GeV.

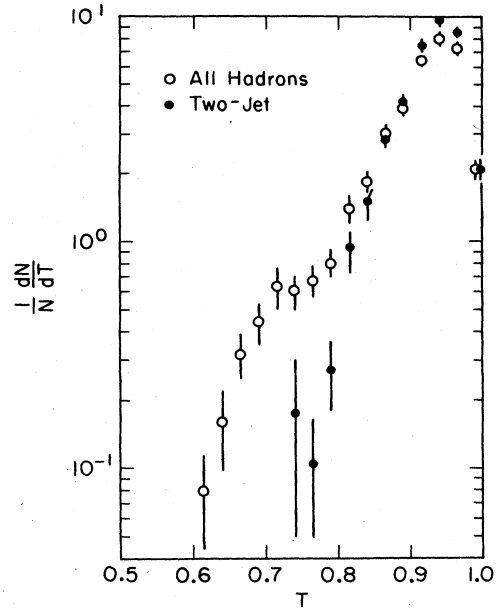

FIG. 11. Thrust distribution for the one-photon-annihilation sample, for both all hadrons (open points) and for the two-jet sample (closed points). The shoulder at $T \sim 0.75$ results from the phase-space cutoff of the radiative tail coming from gluon emission.

energy (26—30 GeV) in Fig. 9(b). These pp data clearly show a narrower sphericity distribution.

Our mean value, $\langle S \rangle = 0.130 \pm 0.003 \pm 0.010$, is shown in Fig. 10, and compared to several other e^+e^- data.[23,24] Below about 5 GeV, the $\langle S \rangle$ values observed are close to those predicted by phase space ($\langle S \rangle \sim 0.4$). As the energy is increased, however, $\langle S \rangle$ decreases rapidly as the particles produced become more and more collimated. A power law $\langle S \rangle = AW^{-B}$, with $A = 1.07 \pm 0.03$ and $B = 0.645 \pm 0.009$, represents the e^+e^- data for $W > 5$ GeV reasonably well, as shown by the line in Fig. 10.

Hadron-hadron measurements of $\langle S \rangle$ as a function of energy for beam jets, also shown in Fig. 10, have a trend similar to the e^+e^- data. The ADCHW data[12] lie systematically below the e^+e^- results as expected from the comparison of Fig. 9(b).

Several bubble-chamber experiments[9–11] at lower energy have also reported sphericity values for beam-jet data. It is not clear how to represent these results on Fig. 10 since the effective c.m. energy is not known for these data samples. We show them as a horizontal band ranging from $W/2$ to W. The latter would be the appropriate energy scale if the leading particles took half of the c.m. energy, which is the case on average. Within this uncertainty, these data also lie below the trend of the e^+e^- results.[25]

Heavy-quark production occurs in about 45% of e^+e^- annihilation events, but is negligible in low-p_T hadronic reactions. To check whether the production of heavy quarks is responsible for this difference in S, we have separated the light-quark (u,d,s) events in our MC program and find only a 10% difference in $\langle S \rangle$ for this set as compared to all the data. Thus, it appears that the heavy-quark production accounts for only a part of the difference between the e^+e^- and pp data.

Some measurements have also been reported from antineutrino interactions.[26] These data, which are at low c.m. energy, agree quite well with the e^+e^- results, as shown by the typical points plotted in Fig. 10.

Although the e^+e^- data are well reproduced by the various MC programs[19] that simulate the elemental QCD parton processes and parametrize the fragmentation process, the similarity of the data from these different reactions means that the global jet measures are not a strong discriminator of the different processes. The event shapes seem to be dominated by longitudinal phase space.

Other measures of the shape of the events are given by the distributions in the thrust and aplanarity variables. In Fig. 11 are shown our measurements of thrust for the one-photon-annihilation sample as well as the two-jet

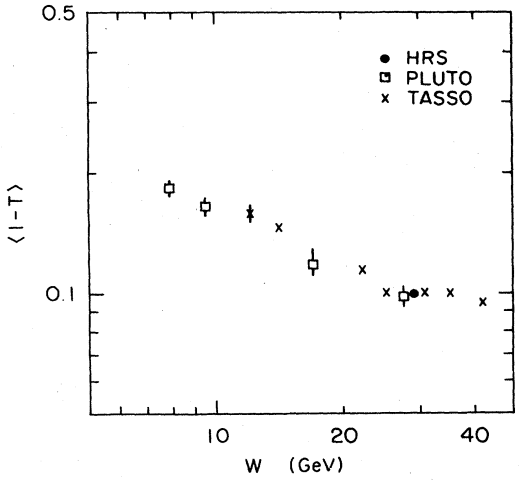

FIG. 12. Energy dependence of $\langle 1-T \rangle$ for e^+e^- annihilation.

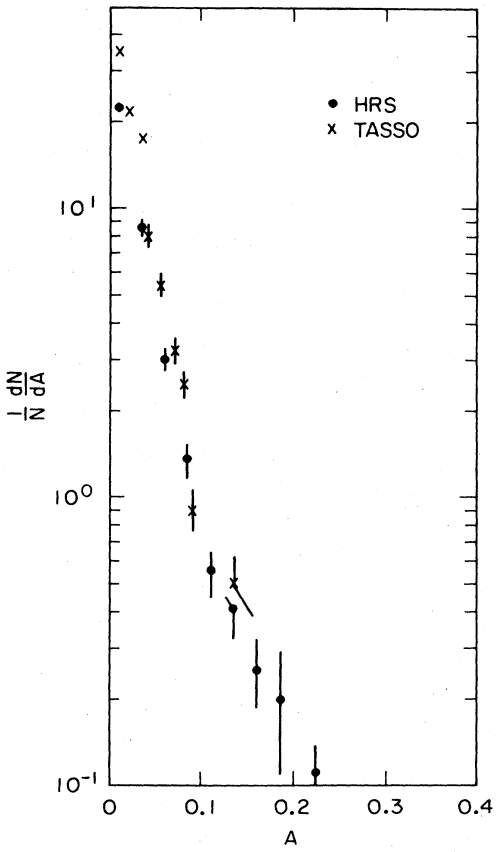

FIG. 13. Aplanarity distribution compared to the TASSO measurements.

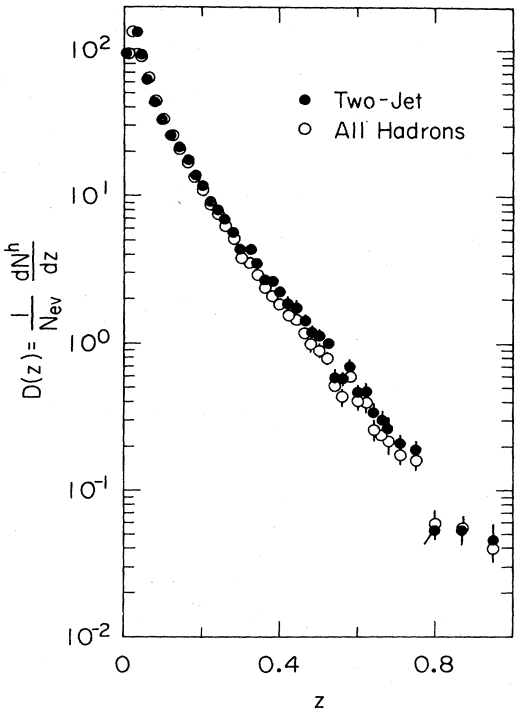

FIG. 14. Fragmentation function, $D(z)=(1/N_{ev})dN^h/dz$, both for the one-photon-annihilation sample (all hadrons, open points) and the two-jet sample (closed points).

sample. The mean value of $\langle 1-T\rangle$ of 0.100 ± 0.002 for the total sample agrees well with other e^+e^- measurements[22–24] as seen in the energy dependence of $\langle 1-T\rangle$ shown in Fig. 12.

The aplanarity distribution, shown in Fig. 13, is in good agreement with the TASSO e^+e^- data at 30 GeV.[22]

Single-particle momentum distributions

Figure 14 shows the fragmentation function distribution $D(z)$ measured both for all events and for the two-jet sample. These distributions are quite similar in overall shape, although the two-jet data lies above the overall sample at high z. This is the expected behavior because of the gluon emission in the total data sample. The data for $z>0.05$ can be represented by the sum of two exponentials:

$$D(z)=A\exp(-Bz)+C\exp(-Dz)\ .$$

The results of the fits are given in Table I.

The scaling of this distribution is illustrated in Fig. 15 where we compare the $W^2d\sigma/dz$ values measured by the TASSO group at 14 and 34 GeV (Ref. 27) with our results for the total data sample. The agreement is excellent in the overlap region. Our data extend to higher z values.

Another measure of the longitudinal evolution of the jets is given by the distribution of the single hadrons within a given jet ordered by their z values. Figure 16 shows the distribution of the highest-, second-highest-, and third-highest-momentum particle within one jet, for our two-jet data sample. The mean values are highest momentum $\langle z\rangle=0.270\pm0.003$, second highest momentum $\langle z\rangle=0.100\pm0.001$, third highest momentum $\langle z\rangle=0.050\pm0.001$.

The invariant distribution, relative to the thrust axis $F(x_F)$, is shown in Fig. 17, both for all events and for the two-jet sample.

Since the fragmentation function is dominated by single-quark-to-meson transitions for large x_F, it should vary as $(1-x_F)^n$, based on dimensional-counting arguments.[28] Including spin, the theoretical expectation is that the distribution for the favored transitions ($u\to\pi^+$, $d\to\pi^-$, etc.) should go as $(1-x_F)^2+\mu^2/Q^2$, where μ^2 is

TABLE I. Fits to the fragmentation function $D(z)=A\exp(-Bz)+C\exp(-Dz)$.

Data sample	z range	A	B	C	D	χ^2/DF
All events	0.04—0.8	195.1±10.2	24.6±1.1	27.3±2.8	8.08±0.14	1.91
Two-jet events	0.04—0.8	216.7±11.4	28.4±1.2	58.4±2.5	7.91±0.12	1.41

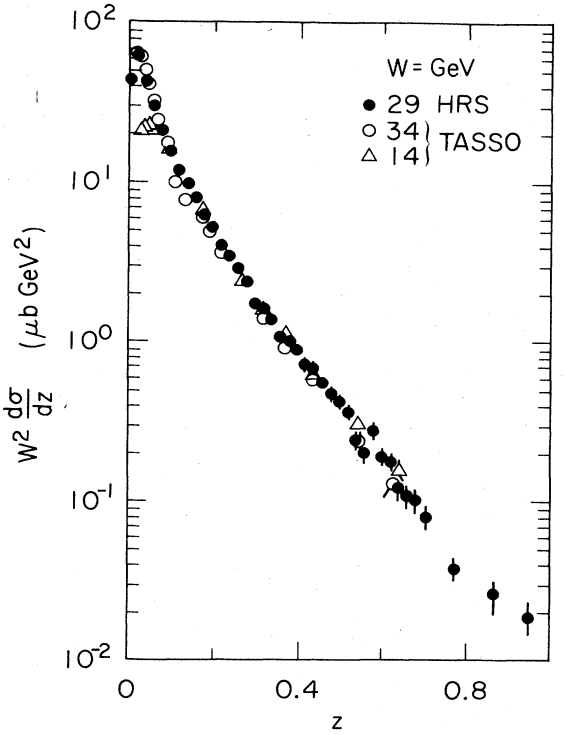

FIG. 15. Comparison of the scaling cross sections $W^2 d\sigma/dz$, for our data at $W=29$ GeV and TASSO measurements at W values of 14 GeV and 34 GeV.

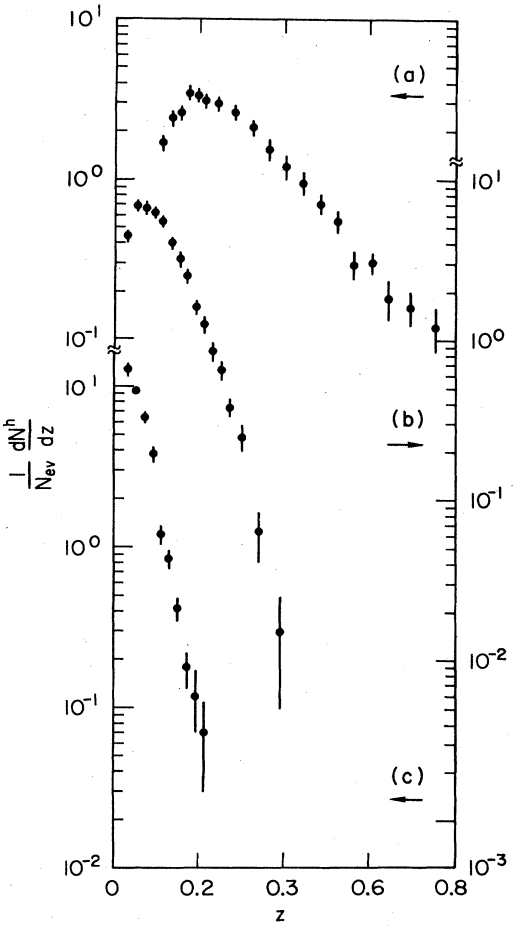

FIG. 16. Momentum fraction z of (a) highest-momentum charged particle (left scale), (b) second-highest-momentum charged particle (right scale), and (c) third-highest-momentum charged particle (left scale) in any one jet for our two-jet data sample.

a constant.[29] Subsequent quark-meson transitions will modify this simple behavior. The unfavored transitions ($u \to \pi^-$, $d \to \pi^+$, etc.) are expected to be much more heavily suppressed with $n \sim 4$—6 since additional spectator quarks are present in these cases. The lower x_F region is also strongly populated by hadrons coming from the decay of heavy particles containing the c and b quarks. Our studies of D-meson production,[30] for example, show that the final π and K mesons from the D decay are largely confined to the low-x_F region. We expect that the high-x_F region measures the behavior of light-quark (u,d,s) fragmentation.

We show in Fig. 18 the $F(x_F)$ distribution for the two-jet sample with logarithmic scales to display better the high-x_F variation of the data. The full line on Fig. 18, which represents the data well, is the result of a simple model. The line is the convolution of a series of quark-meson transitions, each with a $(1-x_F)^2$ variation but with the quark energy appropriately reduced at each stage, This distribution approaches a $(1-x_F)^2$ variation at high x_F (which is shown by the dashed line in Fig. 18). The data is consistent with the expected $(1-x_F)^2$ variation. The data point at $(1-x_F) \simeq 2 \times 10^{-2}$ contains four events and so, although it lies above the extrapolation of a $(1-x_F)^2$ term, we conclude that there is no convincing evidence for the μ^2/Q^2 term at the present statistical level of the data.

It has been known for some time that the fragmentation functions measured in deep-inelastic lepton scattering, in e^+e^- annihilation, and in high-transverse-energy hadron collisions show the universal feature of a steeply falling function. More refined measurements show that the slope for each of these hard processes increases logarithmically with increasing jet energy as the gluon emission causes a softening of the jet.[31]

Fits to νp and $\bar{\nu} p$ data[32] in the range $0.2 < x_F < 1.0$ allow separated measurements of the u- and d-quark fragmentation to π^+ and π^-. The favored processes give n values of ~ 1.5 as compared to ~ 2.5 for the unfavored processes. These results, although spanning a wide x_F range, are in qualitative agreement with our high-x_F data of Fig. 18, since we cannot separate, for example, the $d \to \pi^-$ (favored) from the $u \to \pi^-$ (unfavored) fragmentations, but measure the sum of the two.

Extensive studies have been made of hadronic fragmentation for many different beam particles leading to various secondary particles. For example, measurements made at Fermilab[33] give n values of 3.43 ± 0.11 for $p \to \pi^+$ and 4.53 ± 0.16 for $p \to \pi^-$. These results show a clearly different behavior from our data, even taking into account the increase in slope of our data at lower x_F.

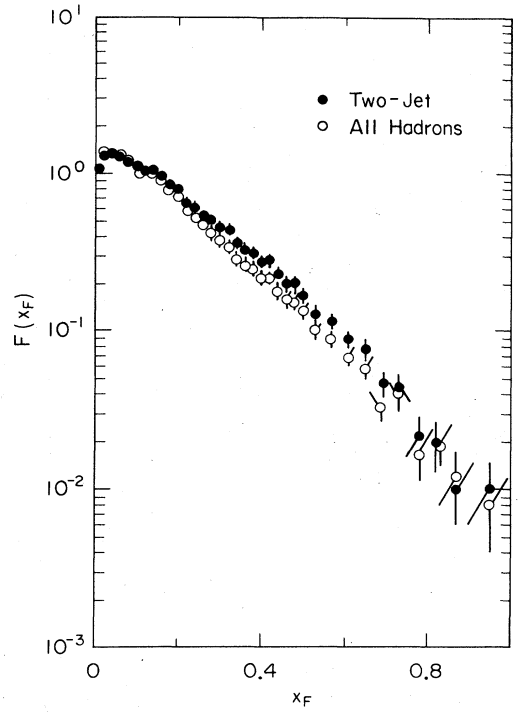

FIG. 17. Invariant Feynman-x distribution, $F(x_F) = (1/\pi)(1/N_{ev})(2E/W)dN^h/dx_F$, for the one-photon-annihilation sample (all hadrons, open points) and the two-jet sample (closed points).

This conclusion may be contrasted to the observation of the BCF collaboration who note that in high-energy pp collisions, if the leading protons are removed and the c.m. energy appropriately reduced, then the remaining particles in the event sample give the same z distribution as is observed in e^+e^- annihilation when the comparison is made at the same effective c.m. energy. We show in Fig. 19(a) such a comparison of the published BCF data[34] for negative-particle production, with our two-jet fragmentation function. The two data sets are in quite good agreement up to $z=0.6$, where the pp data ends. A quantitative comparison at high z could be more revealing of any underlying physics similarities since this is the region that may be amenable to simple interpretation. Of course,

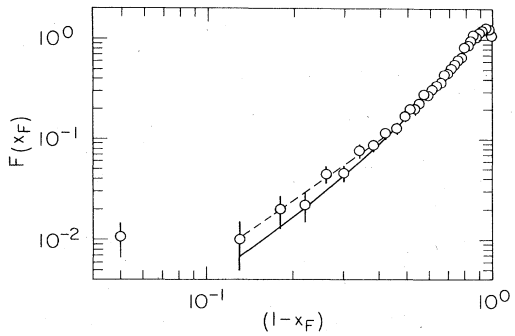

FIG. 18. Invariant Feynman-x distribution $F(x_F)$. The full line shows the result of the simple model discussed in the text. The dashed line shows a $|1-x_F|^2$ variation.

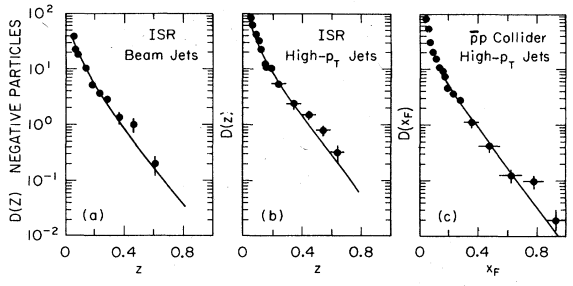

FIG. 19. Fragmentation functions measured for (a) negative particles in beam-jet data from the ISR, (b) high-p_T measurements at the ISR, and (c) high-p_T measurements at the CERN $\bar{p}p$ collider. The lines show the fits to our fragmentation functions in z or x_F as appropriate.

reducing the c.m. energy by the amount carried by the leading protons automatically raises the apparent cross section at the higher-z values. This high-z region is also populated with pions from the decay of diffractively excited subsystems such as $p\pi^+\pi^-$,[35] which is clearly not relevant to any comparison with e^+e^- annihilation.

Fragmentation functions of high-p_T jets, measured in the Axial Field Spectrometer[36] at the ISR and by the UA1 collaboration at the SPS collider,[37] are shown in Figs. 19(b) and 19(c), respectively. The fit to our measured fragmentation function in z or x_F as appropriate are shown as the lines on these figures. The normalization is uncertain since the absolute jet multiplicity is difficult to measure in the high-p_T hadronic experiments. The jet energies are also different in the two cases: ~ 16 GeV for the ISR experiment and ~ 32 GeV for the collider experiment. Both experiments, however, show fragmentation functions in quite good agreement with our data.

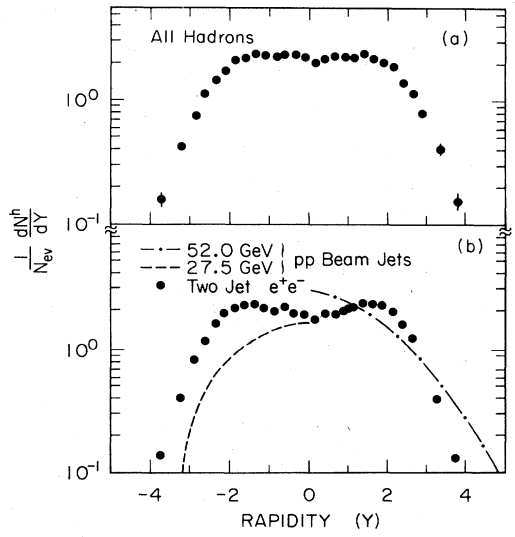

FIG. 20. Rapidity distribution $(1/N_{ev})dN^h/dY$ for (a) the one-photon-annihilation sample (all hadrons) with all particles assigned the pion mass, and (b) the two-jet data after mass corrections. The dashed and dashed-dotted curves on (b) show the measured rapidity distributions for pp beam jets at $W=27.5$ GeV and $W=52$ GeV, respectively.

Rapidity distributions

The corrected rapidity distribution for the one-photon-annihilation sample, shown in Fig. 20(a), has a relatively flat plateau in the central region. This region is populated by the low-momentum tracks that the HRS, with its high magnetic field, detects with lower efficiency. The correction factor at $Y=0$ is about 30%. The full width of the distribution at half height is 5.3 units, and the height of the central region,

$$\frac{1}{N_{\rm ev}}\frac{dN^h}{dY}=2.30\pm0.02\pm0.07\ ,$$

averaged over the Y range, $0.2<|Y|<1.0$.

Since we assigned all particles the pion mass in plotting this rapidity distribution and since this causes heavier particles to move to higher $|Y|$ values, we have calculated a correction factor based on the MC simulation. The two-jet rapidity distribution corrected for this effect is shown in Fig. 20(b). This corrected data still shows the minimum at $Y=0$ and the broad maximum near $|Y|=1.8$.

The dashed curve in Fig. 20(b) shows the rapidity distributions for 405 GeV ($W=27.5$ GeV) pp interactions measured by Bromberg *et al.*[38] in the Fermilab bubble chamber and the dashed-dotted curve shows the distribution measured at 52 GeV at the ISR.[39]

The pp data has a different shape from that measured in e^+e^- annihilations. This difference would be enhanced if the pp diffractive events that populate the lower multiplicities and have a wider Y distribution were removed. We note that the leading protons have been removed in the 405 GeV data, which accounts for the lack of a high-Y tail as compared to the ISR measurements.

Hydrodynamic models[40] give a flat rapidity distribution which is in reasonable agreement with our measurement.

We now compare the energy variation of the height of the rapidity distribution at $Y=0$ in e^+e^- annihilation and pp beam jets. Measurements of the Mark I[41] and the TASSO[42] groups are shown together with data from this experiment in Fig. 21. All the e^+e^- data are averaged over the region $0.2<|Y|<1.0$. The TASSO inclusive rapidity distributions at high energy also decrease slightly in the central rapidity region and the plateau height is in good agreement with our measurement.

The lower data set of Fig. 21 connected by the line show the energy variation of similar measurements from pp interactions.[38] This data extends from c.m.-energy values of a few GeV up to 52 GeV. The recent ISR measurements[39] at $W=52$ GeV seem to be higher than the trend of the bubble-chamber data, although the errors are large. The $\bar{p}p$ collider results at $W=540$ GeV are also shown.[43] The $\bar{p}p$ collider measurements are made using the pseudorapidity variable ($\eta=-\ln\tan\theta/2$). In the central region $d\sigma/dY$ typically exceeds $d\sigma/d\eta$ by 10 to 20%.

Both sets of data show a rapidity distribution with a height of the central region that increases with energy as $\ln W$ although the e^+e^- data lie systematically above the hadron results.[44] This difference is somewhat more than can be adjusted by a simple reduction of the available energy to $W/2$ for the hadronic data. This is illustrated by the dashed-dotted line where we plot the fit to the hadronic data displaced by a factor of 2 in W.

The difference in the plateau heights may reflect an increased multiplicity of soft hadrons from gluon radiation in the e^+e^- events as compared to pp interactions. It may also be connected with the multiplicity of soft hadrons coming from, for example, D- and B-meson decay. This difference is shown in more detail in the comparison of the shapes of the full rapidity distributions discussed earlier.

An alternative way of studying the central region is to look at the very-small-z region, since low-z particles are genuinely soft whereas particles at low Y can have a high momentum if the transverse momentum is large.

This region of the phase space is sensitive to the infrared structure of QCD.[45] An explicit calculation shows a maximum in $zD(z)$ for the gluon at $z\sim(Q_0/W)^{1/2}$

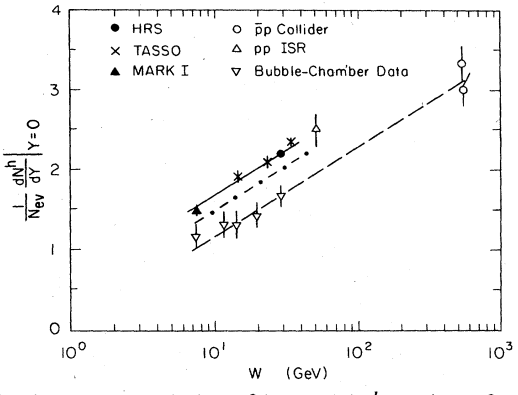

FIG. 21. Energy variation of $(1/N_{\rm ev})dN^h/dY\,|_{Y=0}$ for e^+e^- annihilation compared to pp data. The parallel lines show an $A+B\ln W$ dependence to guide the eye. The dashed-dotted line shows the fit to the pp data plotted at $W/2$.

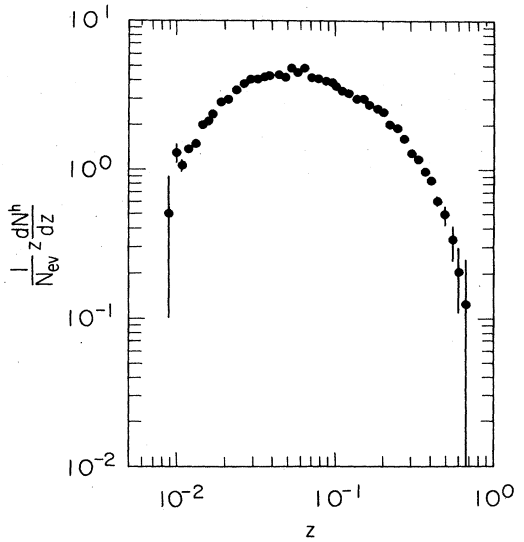

FIG. 22. Fragmentation function shown as $(1/N_{\rm ev})zdN^h/dz$ for e^+e^- annihilation at 29 GeV to illustrate the behavior of the cross section at low z.

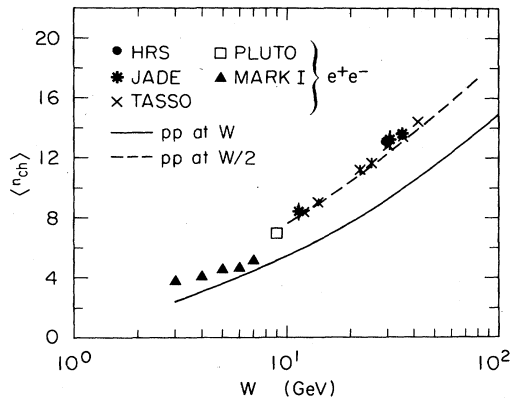

FIG. 23. Mean-charged-multiplicity $\langle n_{ch} \rangle$ measurements in e^+e^- annihilation compared to pp data (solid line). The dashed line shows the fit to the pp data plotted at $W/2$.

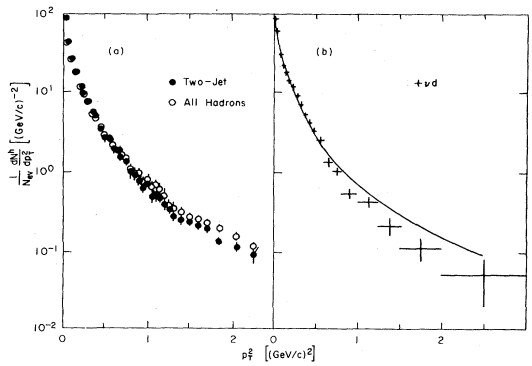

FIG. 24. (a) Distribution in $p_T{}^2$ for e^+e^- annihilation at 29 GeV for the one-photon-annihilation sample (all hadrons, open points) and for the two-jet events (closed points). (b) The curve shows the fit to the $p_T{}^2$ distribution for all hadrons from e^+e^- annihilation at 29 GeV compared to νd measurements in the range 9 GeV $< W <$ 18 GeV.

where Q_0 is the cluster mass cutoff. For a typical value of $Q_0 \sim 0.4$ GeV, this corresponds to the region $z \sim 0.1$. Hadrons that come from the cluster decays will reflect this result but the exact shape of the hadron-z distribution depends on the details of the gluon fragmentation. One guess is that $Q_0 \sim m_\pi$ which corresponds to $z \sim 0.07$.

Our corrected data shown in Fig. 22 agree with this suggested peaking in the range $z = 0.04$–0.06. Our low-momentum cutoff of 0.1 GeV/c truncates the data well below the region where the z fragmentation is maximal, and so does not affect this conclusion.

Mean charged multiplicity

We now compare the energy variation of the mean charged multiplicity $\langle n_{ch} \rangle$ for e^+e^- data and pp data. Our observed multiplicity distribution was corrected by comparing the detected multiplicities of the MC events with the input multiplicities before the detector simulation and track reconstruction was done. The result is $\langle n_{ch} \rangle = 13.10 \pm 0.05 \pm 0.6$ for the total data sample,[46] where the error is dominated by systematic uncertainties.

Figure 23 shows that our measurement is in good agreement with other e^+e^- data.[47] If the pp results[48] represented by the full line in Fig. 23 are plotted at $W/2$ to account for the energy taken in leading particles, then the $\langle n_{ch} \rangle$ values in pp and e^+e^- reactions in the present energy agree with each other (dashed line). This is also the case if the reduced data set selected by removing the highest-momentum particles is used.[49,50] However, the best fit to the e^+e^- data shows a stronger W dependence than does the pp data,[42] so at much higher energies such a simple scaling may not continue.

Transverse distributions

We have also studied the distributions in momentum transverse to the jet axis. The overall distribution in transverse momentum for the one-photon-annihilation events is shown in the $p_T{}^2$ distribution of Fig. 24(a). Such distributions have been fit by an exponential in the transverse mass,[2] $m_T^\pi = (m_\pi{}^2 + p_T{}^2)^{1/2}$ using the equation

$$\frac{1}{N_{ev}} \frac{dN^h}{dp_T{}^2} = A \exp(-B m_T^\pi) .$$

Our fits for different $p_T{}^2$ ranges, which give B values in the range 6.2–6.6, do not have good confidence levels. We have, therefore, fit the distribution with the sum of two terms using a kaon and a pion transverse mass using the equation:

$$\frac{1}{N_{ev}} \frac{dN^h}{dp_T{}^2} = A \exp(-B m_T^\pi) + C \exp(-D m_T^K)$$

with obvious notation. We constrain this fit so that the integrals of the two distributions are in the ratio 5:1, which is approximately the ratio of pions to kaons in e^+e^- annihilation in our energy range. This combined fit gives a satisfactory representation of the data with slopes of $B = 7.10 \pm 0.07$ and $D = 3.03 \pm 0.07$. The results of all of the fits are summarized in Table II.

Qualitatively similar behavior in $p_T{}^2$ is seen in other re-

TABLE II. Fits to the $p_T{}^2$ distribution (see text).

Data sample	$p_T{}^2$ range [(GeV/c)^2]	A	B	C	D	χ^2/DF
All events	0–0.5	329.4±9.9	6.57±0.08			2.9
All events	0–1.0	292.8±7.6	6.24±0.06			3.9
All events	0–2.5	361.5±10.7	7.10±0.07	14.9±0.9[a]	3.03±0.07	0.66

[a]Fixed by 5:1 ratio of π to K mesons.

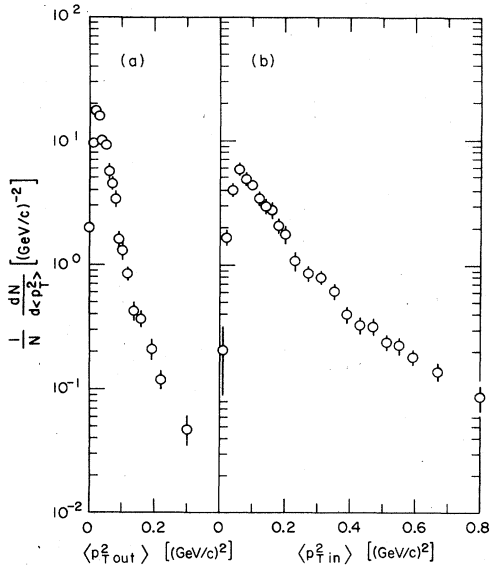

FIG. 25. (a) Distribution in $p_T{}^2$ out of the event plane. (b) Distribution in $p_T{}^2$ in the event plane.

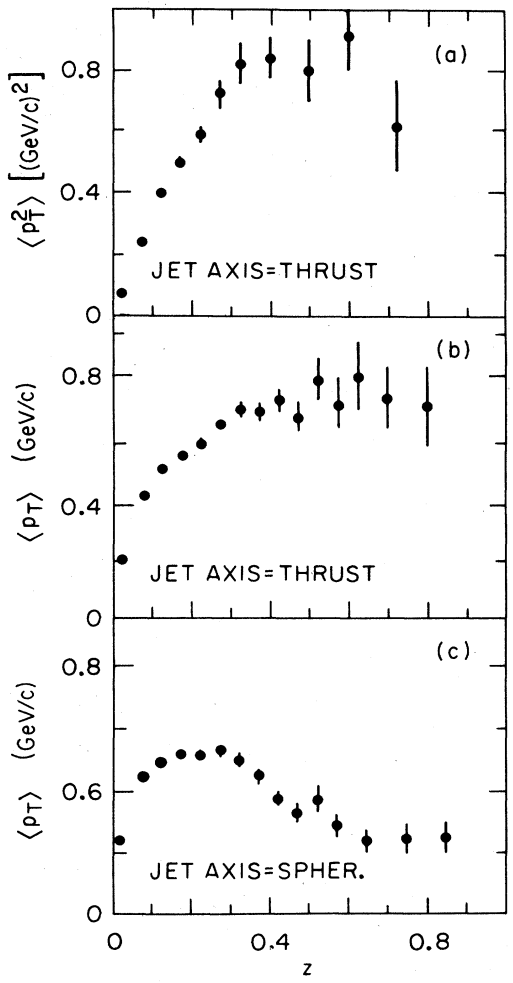

FIG. 26. (a) Distribution in mean of transverse momentum squared $\langle p_T{}^2 \rangle$, measured relative to the T axis, as a function of z. (b) Distribution in mean transverse momentum $\langle p_T \rangle$, measured relative to the T axis, as a function of z. (c) Distribution in mean transverse momentum $\langle p_T \rangle$, measured relative to the S axis, as a function of z.

actions. For example, we show in Fig. 24(b) the measurements of u-quark fragmentation studied in νd interactions.[51] These results in the c.m. energy range 9 GeV $< W <$ 18 GeV, when fit with a single exponential in m_T^{π} give $B = 6.0 \pm 0.2$ (GeV/c)$^{-1}$ and so agree reasonably well with our measurements at low $p_T{}^2$. As seen by the line in Fig. 24(b), our higher-energy e^+e^- measurements lie above the neutrino data in the higher $p_T{}^2$ range. Such an increase in the cross section at high p_T is also observed in the e^+e^- data as the W value is increased.[42]

The events are not symmetric around the jet axis, but develop a definite plane, that is defined by the quarks and hard gluon of reaction (2). Figures 25(a) and 25(b) show the distributions in $(p_{T_{\rm out}})^2$ and $(p_{T_{\rm in}})^2$ normal to the S axis but perpendicular to and parallel to the event plane, respectively. The distribution in the plane is clearly much broader than that out of the plane. Indications of similar behavior have also been seen in μp scattering[52] and in the highest-energy νN interactions.[53]

Our measured mean p_T and $p_T{}^2$ values are shown as a function of z in Fig. 26. We show the $\langle p_T \rangle$ values measured relative to the thrust axis in Fig. 26(b) and to the sphericity axis in Fig. 26(c). Since the latter axis is chosen by minimizing $p_T{}^2$ it is not surprising that the $\langle p_T \rangle$ values decrease in the higher z range when the jet axis is defined by sphericity.

The $\langle p_T \rangle$ values are small at low z as required by the kinematics but grow to plateau values of $\langle p_T \rangle = 0.70 \pm 0.02$ GeV/c and $\langle p_T{}^2 \rangle = 0.82 \pm 0.05$ (GeV/c)^2 for $z > 0.3$ when measured relative to the T axis.

We compare these results in Fig. 27 with measurement of $\langle p_T \rangle$ and $\langle p_T{}^2 \rangle$ in other reactions. Our data are represented by the lines on these plots. Our $\langle p_T \rangle$ values agree at low z, but are higher for $z > 0.1$ than the 205-GeV ($W = 19.6$ GeV) beam-jet measurement of $pp \to \pi^- + X$ made by Kafka *et al.*[38,54] In contrast, the $\langle p_T{}^2 \rangle$ values measured in deep-inelastic muon scattering[55] are in good agreement with our data although the mean c.m. energy is much lower ($\langle W \rangle \sim 14.5$ GeV). Measurements of e^+e^- annihilation at 14 GeV[23] show $\langle p_T \rangle$ values for $z > 0.3$ of ~ 0.4 GeV/c much below the μp data.

We note that our data fall below the μp measurements at low z. This result may be partially instrumental, but may also reflect the influence of the diquark target jet that is present in the lepton-scattering experiment.

These comparisons can be qualitatively understood in terms of the different effects that contribute to the three reactions. The lepton-scattering data has three contributions: (i) a fragmentation p_T, (ii) a QCD contribution from gluon bremsstrahlung, and (iii) the intrinsic transverse momentum K_T of the struck quark in the nucleon target. The latter includes initial-state-gluon effects and

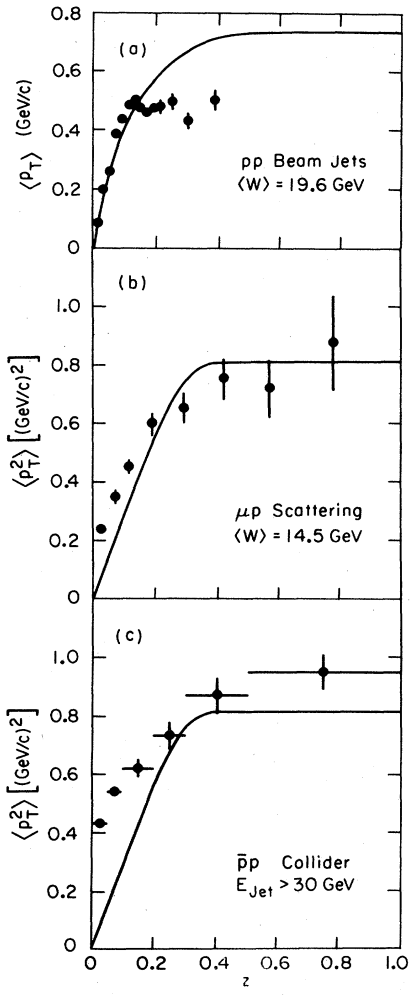

FIG. 27. z variation of (a) $\langle p_T \rangle$ for 205 GeV pp beam-jet data, (b) $\langle p_T{}^2 \rangle$ for μp scattering at $\langle W \rangle = 14.5$ GeV, and (c) $\langle p_T{}^2 \rangle$ for high-p_T hadron jets from the $\bar{p}p$ collider for $E_{\text{jet}} > 30$ GeV. The lines show the shape of the e^+e^- measurements at $W = 29$ GeV.

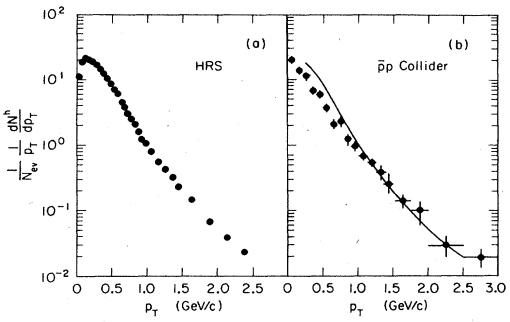

FIG. 28. (a) p_T distribution for e^+e^- annihilation at 29 GeV shown as $(1/N_{\text{ev}})(1/p_T)dN^h/dp_T$. (b) p_T distribution for high-p_T jets at the $\bar{p}p$ collider $[(2/N_{\text{jet}})(1/p_T)dN/dp_T]$. The curve shows the fit to our e^+e^- measurements in the range $0.25 < p_T < 2.5$ GeV/c.

increases as z^2. The hadronic beam-jet data reflect only the fragmentation p_T plus the K_T effect, whereas the e^+e^- data lack the K_T contribution.

In Fig. 27(c) we compare our measurements with high-p_T jet data from the SPS collider. These jets, which are thought to result from gluon fragmentation, give $\langle p_T{}^2 \rangle$ values at high z somewhat higher than we measure, consistent with the higher jet energies involved. The collider data lies much above our measurements at low z. This region for the collider experiment may not be free of particles in the beam jets that have been misassigned to the high-p_T jet.

Finally, we show in Fig. 28(a) our measurement of the transverse distribution

$$\left[\frac{1}{N_{\text{ev}}}\frac{1}{p_T}\frac{dN^h}{dp_T}\right]$$

as a function of p_T. We compare this distribution with the results of the study of high-p_T jets at the SPS collider in Fig. 28(b). The $\bar{p}p$ cross sections are given per jet, and so have been increased by a factor of 2 in the figure. The $\bar{p}p$ data are somewhat broader than our data as indicated by the fit.

CONCLUSIONS

The mean values of various kinematic quantities that we measure for e^+e^- annihilation at 29 GeV are summarized in Table III.

Our measured neutral energy fraction and R value, as well as the thrust and aplanarity distributions for the total annihilation sample, agree well with other data in this energy range. The shape of the jets, measured by the sphericity variable, are broader than beam jets measured in hadron collisions at similar available energies.

The single-particle fragmentation function has the same overall shape as measurements made in high-p_T hadron collisions and in neutrino interactions, but exceeds that for low-p_T pp interactions for the higher z values. Our fragmentation function at high x_F shows an approximately $(1-x_F)^2$ dependence, consistent with theoretical expectations. The central region, as measured by the rapidity distribution, is quite different in e^+e^- annihilation as compared to measurements of low-p_T beam jets. We observe a small central dip, whereas the hadronic data peaks

TABLE III. Mean values of kinematic variables. The first error gives the statistical uncertainty and the second error is our estimate of the systematic uncertainty.

Variable	All hadrons	Two-jet events
S	0.130±0.003±0.010	
$1-T$	0.100±0.002	
A	0.029±0.001±0.002	
z	0.090±0.001	0.944±0.001
x_F	0.081±0.001	0.087±0.001
p_T (GeV/c)	0.380±0.005	0.361±0.006
$p_T{}^2$ [(GeV/c)^2]	0.237±0.010	0.206±0.008
$(p_{T\text{in}})^2$ [(GeV/c)^2]	0.167±0.007	
$(p_{T\text{out}})^2$ [(GeV/c)^2]	0.044±0.002±0.004	

at $Y=0$. The cross section at $Y=0$ is also higher in the e^+e^- data than is measured in hadronic interactions even though the mean charged multiplicities in the two reactions agree if they are compared at equivalent center-of-mass energies.

The events exhibit a planar structure with a larger transverse momentum in the plane of the event than out of the plane. The distribution in $p_T{}^2$ is similar to lower-energy νN data at low $p_T{}^2$ but our e^+e^- data shows a higher cross section at high $p_T{}^2$. The increase of $\langle p_T \rangle$ and $\langle p_T{}^2 \rangle$ with z is similar in several reactions. The values of $\langle p_T \rangle$ and $\langle p_T{}^2 \rangle$ at high z are in qualitative agreement when the different effects contributing to the several reactions are considered.

ACKNOWLEDGMENTS

This work was supported by the U. S. Department of Energy. The experiment would not have been possible without the support of the technical staff of PEP and of the collaborating institutions. This paper is based, in part, on a Ph.D. thesis submitted to Indiana University by G. Baranko, 1983. The work of H. Neal was supported in part by the J. S. Guggenheim Foundation.

---

[a]Present address: Lockheed Missiles and Space Co., Sunnyvale, CA 94086.
[b]Present address: University of Colorado, Boulder, CO 80309.
[c]Present address: Ecole Polytechnique, Palaiseau, France.
[d]Present address: Bell Laboratories, Naperville, IL 60566.
[e]Present address: MCI Corporation, Washington, DC 20036.
[f]Present address: University of Michigan, Ann Arbor, MI 48109.
[g]On leave of absence from Istituto Nazionale di Fisica Nucleare, Pisa, Italy.
[h]Present address: University of Wisconsin, Madison, WI 53706.
[i]Visitor from Aakayama Medical College, Japan.
[j]Present address: LeCroy Research Systems, West Valley, NY.
[k]Present address: Rutherford Appleton Laboratory, Oxon, England.
[l]Present address: LAPP, Annecy-le-Vieux, France.
[m]Present address: State University of New York, Stony Brook, NY 11973.
[n]Present address: CERN, CH-1211 Geneva 23, Switzerland.
[o]Present address: Laboratory of Nuclear Studies, Cornell University, Ithaca, NY 14853.
[p]Present address: University of Toronto, Toronto, Canada.
[q]Present address: Intel Corporation, Palo Alto, CA 94305.
[r]Present address: Stanford Linear Accelerator Center, Stanford, CA 94305.
[s]Present address: Argonne National Laboratory, Argonne, IL 60439.

[2]L. Foa, Phys. Rep. **22**, 1 (1975); G. Giacomelli and M. Jacob, *ibid.* **55**, 1 (1979).
[3]For a review, see for example, G. Wolf in *Proceedings of the 21st International Conference on High Energy Physics, Paris, 1982,* edited by P. Petiau and M. Porneuf [J. Phys. (Paris) Colloq. **43**, C3-525 (1982)].
[4]G. Kramer, *Theory of Jets in Electron-Positron Annihilation* (Springer Tracts in Modern Physics No. 102) (Springer, Berlin, 1984).
[5]M. Banner *et al.,* Phys. Lett. **118B**, 203 (1982); G. Arnison *et al., ibid.* **123B**, 115 (1983).
[6]R. Horgan and M. Jacob, Nucl. Phys. **B179**, 441 (1981).
[7]L. Van Hove and S. Pokorski, Nucl. Phys. **B86**, 243 (1975); W. Ochs, *ibid.* **B118**, 397 (1977); K. P. Das and R. C. Hwa, Phys. Lett. **68B**, 459 (1977); R. C. Hwa and R. Roberts, Z. Phys. C **1**, 81 (1979); B. Andersson, G. Gustafson, and C. Peterson, Phys. Lett. **69B**, 221 (1977); **71B**, 337 (1977); A. Capella, U. Sukhatme, and J. Tran Thanh Van, Z. Phys. C **3**, 329 (1980).
[8]M. Basile *et al.,* Nuovo Cimento **79A**, 1 (1984), and references cited therein.
[9]R. Göttgens *et al.,* Z. Phys. C **11**, 189 (1981); Nucl. Phys. **B178**, 39 (1981).
[10]M. Barth *et al.,* Nucl. Phys. **B192**, 289 (1981).
[11]D. Brick *et al.,* Phys. Lett. **103B**, 241 (1981); Z. Phys. C **15**, 1 (1982).
[12]A. Breakstone *et al.,* Z. Phys. C **11**, 203 (1981).
[13]J. Whitmore and M. Derrick, Phys. Lett. **50B**, 280 (1974).
[14]Preliminary results have been presented: M. Valdata-Nappi (HRS Collaboration), in *Proceedings of the XIV International Symposium on Multiparticle Dynamics, Granlibakken, Lake Tahoe, California, 1983,* edited by P. Yager and J. F. Gunion (World Scientific, Singapore, 1983), p. 75.
[15]R. Brandelik *et al.,* Phys. Lett. **86B**, 243 (1979); Ch. Berger *et al., ibid.* **86B**, 418 (1979); W. Bartel *et al., ibid.* **91B**, 142 (1980); D. P. Barber *et al., ibid.* **108B**, 63 (1982).
[16]D. Bender *et al.,* Phys. Rev. D **30**, 515 (1984).
[17]J. Ellis *et al.,* Nucl. Phys. **B111**, 253 (1976). These variables are defined as

$$S=\tfrac{3}{2}\min\frac{\sum_i (p_T^i)^2}{\sum_i (p^i)^2},\quad 0\le S\le 1,$$

$$T=\max\frac{\sum_i |p_L^i|}{\sum_i |p^i|},\quad 0.5\le T\le 1,$$

where p_L^i and p_T^i are the transverse and longitudinal momenta of the ith particle with respect to the jet axis and the sum extends over all charged particles. The aplanarity is the normalized momentum squared out of the event plane.
[18]In our simulation the primary partons are generated according to the Lund model and the fragmentation of the partons into hadrons uses the Field and Feynman prescription (see Ref. 19).
[19]R. D. Field and R. P. Feynman, Nucl. Phys. **B136**, 1 (1978); P. Hoyer *et al., ibid.* **B161**, 349 (1979); B. Andersson, G. Gustafson, G. Ingelman, and T. Sjostrand, Phys. Rep. **97**, 32 (1983); R. Odorico, Nucl. Phys. **B172**, 157 (1980); G. Preparata and G. Valenti, *ibid.* **B183**, 53 (1981); R. D. Field and S. Wolfram *ibid.* **B213**, 365 (1983); T. Gottschalk, *ibid.* **B214**, 201 (1983); B. Webber, *ibid.* **B238**, 492 (1984).
[20]S. Clearwater, Ph.D. thesis, Stanford University, 1983; B. Heltsley, Ph.D. thesis, University of Wisconsin, 1983.
[21]W. Bartel *et al.,* Z. Phys. C **9**, 315 (1981).
[22]R. Brandelik *et al.,* Phys. Lett. **94B**, 437 (1980).

[23]G. Hanson *et al.*, Phys. Rev. Lett. **35**, 1609 (1975); Ch. Berger *et al.*, Z. Phys. C **12**, 297 (1982).

[24]M. Althoff *et al.*, Z. Phys. C **22**, 307 (1984).

[25]Brick *et al.* (Ref. 11) also measure $\langle S \rangle = 0.201 \pm 0.006$ for a sample of data in which the leading particle has been removed. The mean available energy for this data is 12.12 GeV. This data point lies above the other hadronic data which again points up the difficulties of interpreting the hadronic experiments.

[26]M. Derrick *et al.*, Phys. Lett. **88B**, 177 (1979); J. P. Berge *et al.*, Nucl. Phys. **B202**, 16 (1982).

[27]R. Brandelik *et al.*, Phys. Lett. **114B**, 65 (1982).

[28]J. F. Gunion, in *Proceedings of the Xth International Symposium on Multiparticle Dynamics, Bruges, Belgium, 1980,* edited by E. DeWolf and F. Verbeure (University of Antwerp, Antwerp, Belgium, 1980), D. Sivers, Annu. Rev. Nucl. Part. Sci. **32**, 149 (1982).

[29]G. R. Farrar and D. R. Jackson, Phys. Rev. Lett. **35**, 1416 (1975).

[30]S. Ahlen *et al.*, Phys. Rev. Lett. **51**, 1147 (1983).

[31]J. F. Patrick *et al.*, Phys. Rev. Lett. **49**, 1232 (1982).

[32]M. Derrick *et al.*, Phys. Rev. D **24**, 1071 (1981); P. Allen *et al.*, Nucl. Phys. **B214**, 369 (1983). The latter collaboration fitting the x_F distribution over the extended range $0.2 < x_F < 1$ find the following results:

Fragmentation	n value
$u \to \pi^+$	1.43 ± 0.08
$d \to \pi^-$	1.49 ± 0.15
$u \to \pi^-$	2.49 ± 0.17
$d \to \pi^+$	2.65 ± 0.24

Clearly at high enough x_F values the favored fragmentation will dominate.

[33]D. Cutts *et al.*, Phys. Rev. Lett. **43**, 319 (1979).

[34]M. Basile *et al.*, Nuovo Cimento **65A**, 414 (1981).

[35]M. Derrick *et al.*, Phys. Rev. D **9**, 1215 (1974).

[36]D. Lissauer (Axial Field Spectrometer Collaboration), in *Proceedings of the 11th SLAC Summer Institute on Particle Physics, 1983,* edited by P. M. McDonough (SLAC, Report No. 267, 1983).

[37]G. Arnison *et al.*, Phys. Lett. **132B**, 223 (1983).

[38]W. H. Sims *et al.*, Nucl. Phys. **B41**, 317 (1972); V. A. Bumazshnov *et al.*, Phys. Lett. **50B**, 283 (1974); C. Bromberg *et al.*, Nucl. Phys. **B107**, 82 (1976); T. Kafka *et al.*, Phys. Rev. D **16**, 1261 (1977).

[39]A. Breakstone, Phys. Lett. **132B**, 458 (1983).

[40]H. Banerjee, A. Biswas, and T. De, Z. Phys. C **14**, 111 (1982).

[41]G. C. Hanson, in *Gauge Theories and Leptons,* proceedings of the XIII Rencontre de Moriond, 1978, edited by J. Tran Thanh Van (Editions Frontières, Gif-Sur-Yvette, 1978), p. 15.

[42]P. Mattig, DESY Report No. 83-038 (unpublished). See also Ref. 24.

[43]K. Alpgard *et al.*, Phys. Lett. **107B**, 310 (1981); **107B**, 315 (1981); G. Arnison *et al.*, *ibid.* **123B**, 108 (1983).

[44]G. W. van Apeldoorn *et al.* [Phys. Lett. **115B**, 55 (1982)] show that at $W = 4.8$ GeV, the rapidity distribution for $\bar{p}p$ annihilation data is higher at $Y = 0$ than e^+e^- at the same low energy. In this case, all the annihilation energy goes into particle production and the gluon effects in e^+e^- annihilation are known to be small.

[45]G. Marchesini and B. R. Webber, Nucl. Phys. **B238**, 1 (1984); A. Bassetto, M. Ciafaloni, and G. Marchesini, Phys. Rep. **100**, 202 (1983). These authors point out that the ordering of the angles of the successive gluon emissions expected in QCD leads to the prediction of a dip at $Y = 0$ although at energies considerably higher than our experiment. In addition, the multiplicity distribution is expected to be broader than a Poisson distribution, which is not in accord with data. See also L. V. Gribov, E. M. Levin, and M. G. Ryskin, *ibid.* **100**, 1 (1983).

[46]Removing the charged particles from K^0 and Λ decay reduces $\langle n_{\rm ch} \rangle$ to 11.7. In principle, the additional charged particles coming from the weak decays of the mesons and baryons containing the c and b quarks should also be removed in arriving at a true primary multiplicity. The hard fragmentation of such heavy quarks, however, means that the remaining available energy would be $\sim W/2$ for the c quark and even less for the b quark. We therefore do not try to make such a correction.

[47]Ch. Berger *et al.*, Phys. Lett. **81B**, 410 (1979); R. Brandelik *et al.*, *ibid.* **89B**, 418 (1980); W. Bartel *et al.*, Z. Phys. C **20**, 187 (1983).

[48]W. Thome *et al.*, Nucl. Phys. **B129**, 365 (1977).

[49]M. Basile *et al.*, Nuovo Cimento **65A**, 400 (1981).

[50]In neutrino interactions, the multiplicity in the forward hemisphere that results from quark fragmentation exceeds that in the backward hemisphere that is populated by the diquark breakup [M. Derrick *et al.*, Phys. Rev. D **25**, 624 (1982); P. Allen *et al.*, Nucl. Phys. **B181**, 385 (1981)]. Good agreement with all the mean multiplicity data has been obtained by M. Bardadin-Otwinowska *et al.* [Z. Phys. C **13**, 83 (1982)] in a model in which the e^+e^- data is represented by $\langle n_{\rm ch} \rangle e^+e^- = 2\langle n_q \rangle$, the neutrino data by $\langle n_{\rm ch} \rangle \nu = \langle n_q \rangle + \langle n_{qq} \rangle$, and the nondiffractive pp data by $\langle n_{\rm ch} \rangle pp = 2\langle n_{qq} \rangle$. The difference between the multiplicities of the quark and diquark fragmentation can be explained by the leading nucleons that are present in the diquark case.

[51]T. Kitagaki *et al.*, Phys. Lett. **97B**, 325 (1980). These authors show that the $\langle p_T^2 \rangle$ value, measured for the quark breakup in νd interactions at $W \sim 16$ GeV, is 0.25 $(\text{GeV}/c)^2$ relative to the known current direction, whereas it is ~ 0.17 $(\text{GeV}/c)^2$ when measured relative to the thrust axis. This is presumably a result of the selection of the thrust direction, but it points up an obvious difficulty in comparing lepton-scattering data with e^+e^- data. See also P. Allen *et al.*, Nucl. Phys. **188**, 1 (1981).

[52]J. J. Aubert *et al.*, Phys. Lett. **130B**, 118 (1983).

[53]H. C. Ballagh *et al.*, Phys. Rev. Lett. **47**, 556 (1981).

[54]The z values of this data are calculated using the full c.m. energy of $W = 19.6$ GeV. Since the effective W value is about half of this value, the data could also be displayed at z values twice as large. This change would not effect the plateau height.

[55]J. J. Aubert *et al.*, Phys. Lett. **95B**, 306 (1980).